ADVANCED MATERIALS TECHNOLOGIES
www.advmattechnol.d

3D Printed Random Lasers

*Yun-Tzu Hsu, Yen-Yu Lin, Yi-Zih Chen, Hsia-Yu Lin, Yu-Ming Liao, Cheng-Fu Hou, Min-Hsuan Wu, Wei-Ning Deng, and Yang-Fang Chen**

3D printing technology sparks a paradigm shift in one-step production, mass customization, and waste minimization. Of late, tremendous advances have been made in 3D printing research, including electronic components, energy-storage gadgets, and medical therapeutic widgets. Lasers with enormous applicable values, ranging from information communication, to health treatment, to industrial manufacturing, have pervasively penetrated and significantly contributed to modern society. However, until now, the platform of 3D printed lasers is absent in all published work. Here, 3D printing technique endowed with great versatility and accessibility allows the possibility to export any desired laser item free from geometrical restraints, constitutional constraints, and skill limitations. Furthermore, based on the biodissolvability, biodegradability, and biocompatibility of the filament, customized 3D printed random laser devices for speckle-free bioimaging and large-scale phototherapy are constructed to investigate inherent multistructures and multifunctional biological systems, providing an excellent solution for intriguing yet challenging issues from extremely complicated groups. It is envisioned that 3D printed random lasers will pave the way for a series of long-anticipated proofs of concept, such as full-field imaging implants, microfluidic laser sensors, and photonic circuit systems.

3D printing is on track to move into a truly transformative technology from design through operation. Additive manufacturing allows 3D items to be fabricated in a "bottom-up" fashion without subtraction (e.g., cutting and shearing) and formation (e.g., assembling and molding), leading to one-step production, maximum material utilization, and minimum expense, in stark contrast to traditional methods. Direct printing by computer-aided design[1,2] boosts mass customization and lessens operation errors; even a layman can formulate any desired products free from geometrical constraints, constitutional restraints, and skill limitations. Inspired by the idea of online-distributed blueprints and localized production, the public can download digital prototypes from the cloud, modify models to fit their needs, and construct real devices anywhere, promising a world where globally shared information and decentralized productions redefine the boundaries of scientific technology. Of late, such an economical, customizable, and publicized invention has been applied to a myriad of applications including sensors,[3–5] transistors,[6] solar cells,[7,8] bioimaging devices,[9] microfluidics,[10–12] integrated smart systems,[13–15] etc.

The exponential growth in laser knowledge fuels the dissemination and penetration of laser-based equipment in modern times, spanning from information communication, health treatment, industrial manufacturing, to scientific research. However, assimilating conventional lasers to the 3D printing arena is quite challenging due to the stringent criteria of rigid resonant cavities with meticulous fabrications and specialized components. Here, random laser systems can serve as a potential alternative. Random laser behavior is achieved when the photons trapped and scattered by the disordered environment stimulate sufficient optical feedback and let the gain surpass the loss.[16–18] Without the necessity of fixed resonators, such cavity-free lasers can be more suitably fabricated by 3D printing technique without onerous and lengthy procedures. Significant efforts have been dedicated to broadening the scope of the material pool of random lasers from inorganic/organic to biological systems,[16,17,19–22] throwing off the shackles from specific and scarce materials. Due to the random scattering mechanism, two exclusive superiorities, laser-level intensity and angle-free emissions, evince high suitability in several fields, including high-lumen illuminants, wearable sensing devices, implantable bioimaging widgets, and interactive photonic lab-on-a-chip systems.[23–27] Integrated with additive manufacturing, it is believed that such an unconventional laser system will be very useful to extend the application of 3D printing technology.

In this work, we successfully design, fabricate, and demonstrate the first 3D printed random lasers (**Figure 1**). As the pioneer and funder of the 3D printed random laser filament (RLF), we selected readily available materials, poly(vinyl alcohol) (PVA), stilbene 420 (S420), and TiO_2 particles, to serve as the printable matrix and random laser media, guaranteeing the accessibility of this approach for the public. Based on the unique mechanism and exceptional physical properties of the RLF, even the simplest prototype, which can be further transformed into any item, can perform pronounced and stable laser

Y.-T. Hsu, Y.-Y. Lin, Y.-Z. Chen, H.-Y. Lin, Y.-M. Liao, C.-F. Hou, M.-H. Wu, W.-N. Deng, Prof. Y.-F. Chen
Department of Physics
National Taiwan University
Taipei 106, Taiwan
E-mail: yfchen@phys.ntu.edu.tw

The ORCID identification number(s) for the author(s) of this article can be found under https://doi.org/10.1002/admt.201900742.

DOI: 10.1002/admt.201900742

Figure 1. 3D printed random lasers with an iconic sample.

behavior. We validate diversified 3D printed devices to investigate the biological system, which is one of the most intricate yet complicated groups to be mimicked or explored due to intrinsically multiscale structures and multifunctional integration. Such a versatile platform will continue inspiring various fields, including in vivo laser imaging gadgets, microfluidic laser sensors, laser therapeutic devices, and photonic circuit systems.[28–31]

To vastly expand the capabilities of 3D printing, shifting from prototyped structures to end-use devices, more types of printing formulae are in urgent need. Until now, several 3D printing platforms have been established such as conductive thermoplastic fused fiber for electronic circuits,[32] graphene-based printable matrix for energy-storage components,[33] and viscoelastic ink formula for biomedical devices.[34] However, there has been no paradigm for optics, especially for lasers. In this research, among different additive manufacturing methods including fused deposition modeling (FDM), selective laser sintering, inkjet modeling, and stereolithography, we chose FDM to set up the scheme for 3D printed random laser systems due to short printing time and safe operation.[35,36] In addition, FDM is capable of processing a wide variety of materials, including metals, polymers, and organic dyes. In order to spread and promote this innovation, easily accessible materials including PVA, S420, and TiO_2 particles were singled out to construct the RLF for FDM.

Figure 2 shows the process of formulating the RLF from the very beginning, and each stage is clearly displayed. First, the random laser materials, S420 and TiO_2 particles, and the thermoplastic matrix, PVA, were mixed together through the mixer, and heated in the hopper dryer to reduce the humidity. Next, the dry mixture was loaded into the main part of the extruder, stirred by a single screw drive auger, and heated at 180 °C until phase transition occurred and the mixture turned to the fused state. The fused mixture was extruded by a tractor to feed through a conduit to the heated nozzle, and the diameter of the filament was determined by manipulating the speed of extrusion. To further cool and solidify, the filament was sent through an air-cooling tunnel. Finally, the filament was examined by a laser micrometer to monitor the diameter, and it was collected as a roll. Although manufacturing the filament required a series of complex stages and caused much difficulty in optimizing considerable parameters, we overcame these adversities and truly realized RLF.

Figure 3a shows the photograph of the extruded RLF with the diameter of 1.75 mm. Due to exceptional chemical stability, outstanding efficiency, and competitive cost, S420 is selected from various laser dyes as the active media of random laser. The disordered distribution of TiO_2 particles and high refractive index contrast between TiO_2 (n = 2.6) and PVA (n = 1.5) enhance photon scattering and thus induce random laser action. To serve as effective scatters, the size of TiO_2 should be comparative with the wavelength of random lasing about hundred nanometers.[37,38] Randomly distributed TiO_2 particles were revealed in the scanning electron microscope (SEM) image (Figure 3b), and the size of the TiO_2 particles is within the range from 200 to 300 nm. In addition, the photoluminescence spectrum of the RLF is exhibited in Figure 3c with the broadband emission centered at 450 nm; the inset shows the photograph of the illuminated filament. As the first demonstration of laser filament, we also compared the basic properties of RLF with other filaments. Most systems need to be fabricated and operated with rigorous requirements due to toxicity and irritant odor, leading to the necessity of extra specialized equipment and increment of hazard during extrusion. Conversely, due to the physical composition of PVA, it is nontoxic and even biocompatible; this

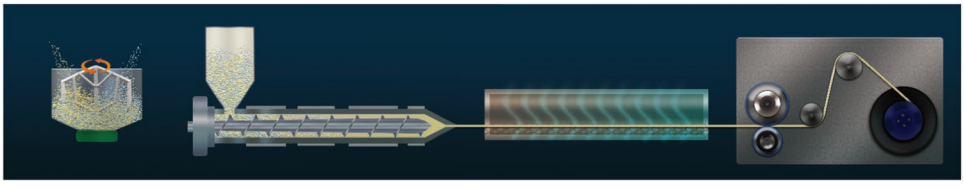

Figure 2. Manufacturing process of 3D printed random laser filament.

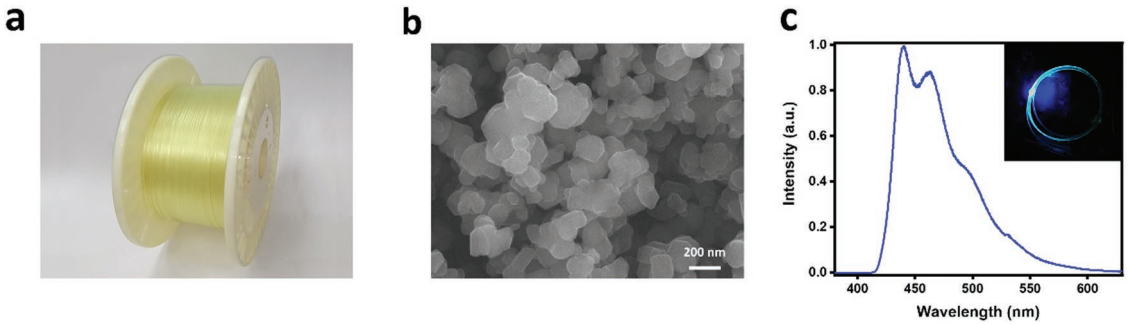

Figure 3. Materials properties of the 3D printed random laser filament (RLF). a) Photograph of the RLF. b) Scanning electron microscope (SEM) image of TiO_2 particles. c) Photoluminescence spectra and corresponding photograph of illuminated RLF.

enhances accessibility for most 3D printers without additional setups and ensuring a safer working environment (Figure S1, Supporting Information).

Random laser behavior is achieved when incident photons are scattered by disordered arrangement of scattering media and provide sufficient optical feedback for the gain surpassing the loss.[16,18,39] Once the recurrently scattered photons form particular paths, the stimulated emission dominates and thus the lasing action is induced. For RLF itself and RLF-based printed devices, while the S420 serves as laser gain media, TiO_2 particles play the role of scattering centers. The lasing characteristics are shown in **Figure 4**. In our study, the 3D printed random laser sample with the length, width, and thickness of 4 cm, 2 cm, and 0.4 mm, respectively, was mounted and pumped on the *xyz*-axis adjustable stage, and the emitted lasing signal was collected by a charge-coupled device (CCD) camera composed of a set of optical lenses, including an extender lens and a focusing lens (Figure S2, Supporting Information). The

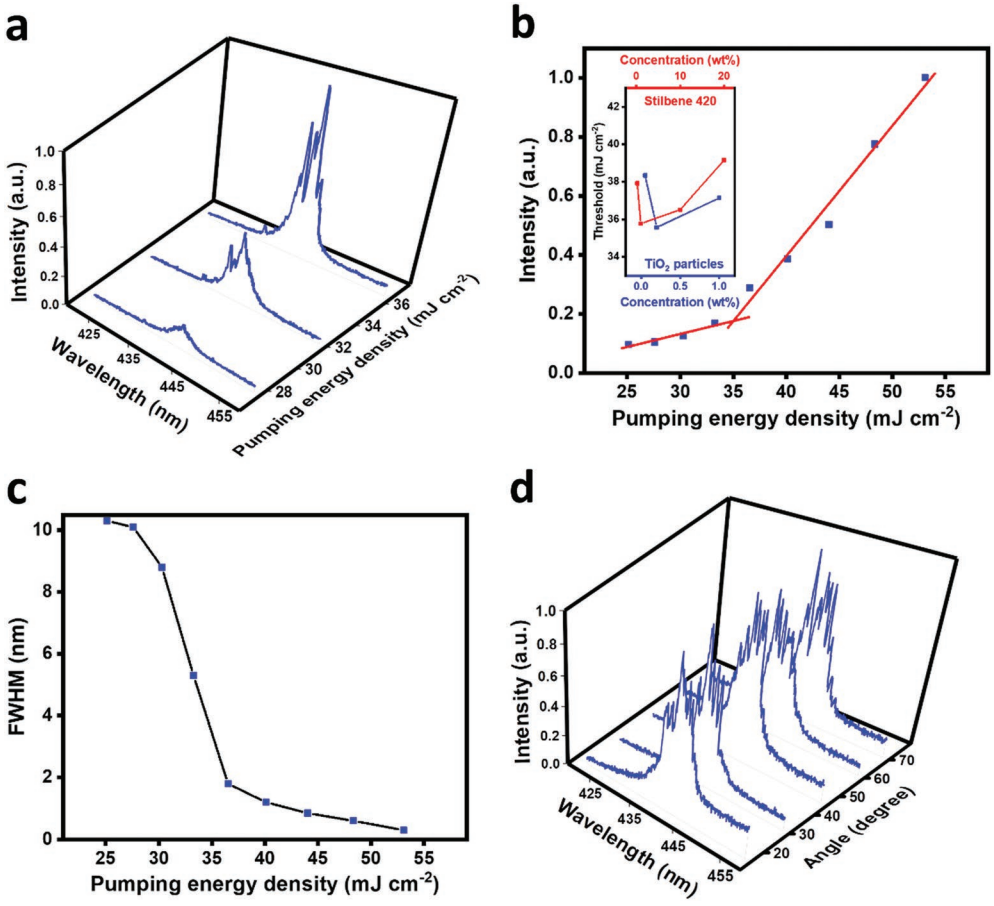

Figure 4. Performance of 3D printed random lasers. a) Emission spectra under different pumping energy density. b) Light-in–light-out curve with the inset showing the random laser threshold at different concentrations of stilbene 420 and TiO_2 particles. c) Full width at half maximum (FWHM) as a function of pumping energy density. d) Angle-independent random laser spectra.

recorded output lasing spectra under different input pumping energy density (PED) are exhibited in Figure 4a. At first, only a broad photoluminescence viewed as spontaneous emission can be observed with PED at 28 mJ cm^{-2}. As the input PED increases to 32 mJ cm^{-2}, the weak perturbation on the top of the spectrum appears, implying the sprouting lasing signal. Multiple spikes resultant from strong optical feedback with multiple loops occur when the PED reaches 36 mJ cm^{-2}, indicating the attainment of laser action. To further analyze the threshold of laser actions, we extracted the maximum lasing intensity with the corresponding PED, as presented in Figure 4b. With linear fitting, an obvious discontinuity can be found with a PED of around 35 mJ cm^{-2}, suggesting the existence of laser threshold. As the PED is below the laser threshold, the intensity of the emission is relatively weak and rises moderately. After increasing PED above the laser threshold, the laser output was abruptly boosted. More details about the optimization of the random laser materials are shown by the inset of Figure 4b. When the concentration of TiO_2 particles is too high, the aggregation of scatterers will ruin the disordered environment and deteriorate the laser performance. For the concentration of TiO_2 particles below 0.05 wt%, the scattering centers are far from enough to induce sufficient photon scattering, and it is hard to trigger the random lasing action. The laser threshold reaches the optimized region at the concentration of stilbene 420 within the range from 1 wt% to 10 wt%. For the concentration below 0.2 wt%, the gain media is not sufficient for random lasing. Figure 4c provides the full width at half maximum (FWHM) of laser performance. When the threshold was attained, lasing was shown with a recognizably steep drop of FWHM from several nanometers to sub-nanometers. Due to the nature of random scattering, the laser output is spatially incoherent, implying an angle-free emission, which is one of the most distinct features of random laser systems. Figure 4d displays the lasing spectra measured with a fixed PED at different angles. (More details about the measurements are provided in the Experimental Section.) The similar lasing performance, including the intensity, linewidth, and wavelength, shows angle independence. All the results shown in Figure 4 can be identified as typical random laser behavior and are in good agreement with random laser theories.[16–18] By manufacturing several molds with different curvatures, fixing our 3D printed samples onto the curved molds seamlessly, and shaping our samples, we also discuss the flexibility of the 3D printed sample and the results are provided in Figure S3 (Supporting Information). By successfully constructing a 3D printed laser optics platform, we have identified one of the missing pieces of 3D printing technology and brought forward great opportunities for laser devices.

In order to unravel the various and sundry facets of living beings, considerable endeavors have been dedicated to bioimaging, from quickly grasping a glimpse of tissue morphology to rigorously scrutinizing cellular mechanisms.[40,41] As shown in **Figure 5**, we demonstrate the prototype of 3D printed random laser implants (RLIs) for bioimaging with biocompatible properties, providing an advantageous route for high-luminance speckle-free image. The design is presented in Figure 5a in the visualization of a stereolithography (STL) file, which can be further converted into a G-code file and read by a 3D printer; Figure 5b is the printed result. Since the size of 3D printed

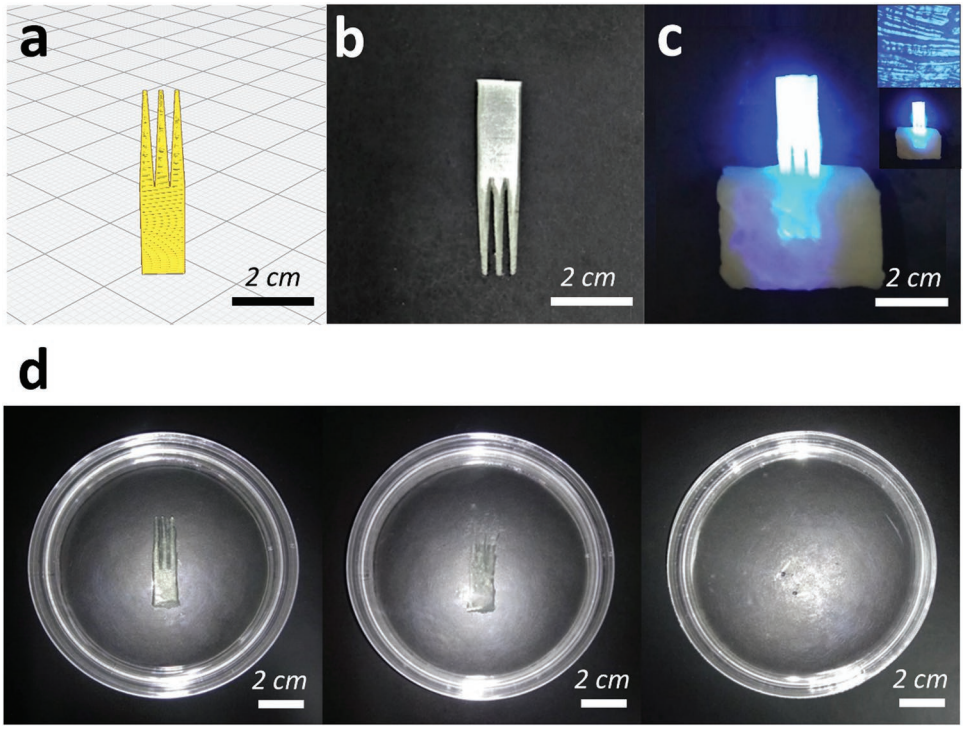

Figure 5. Demonstration of 3D printed random laser implants (RLIs). a) Design of the RLI in the visualization of an STL file. b) Photograph of the 3D printed RLI. c) Laser emissions of the RLI with the top inset showing the microscopic speckle-free image of chicken tissue and the bottom inset exhibiting the random laser emissions with higher PED. d) Photographs at different dissolving stages of the RLI.

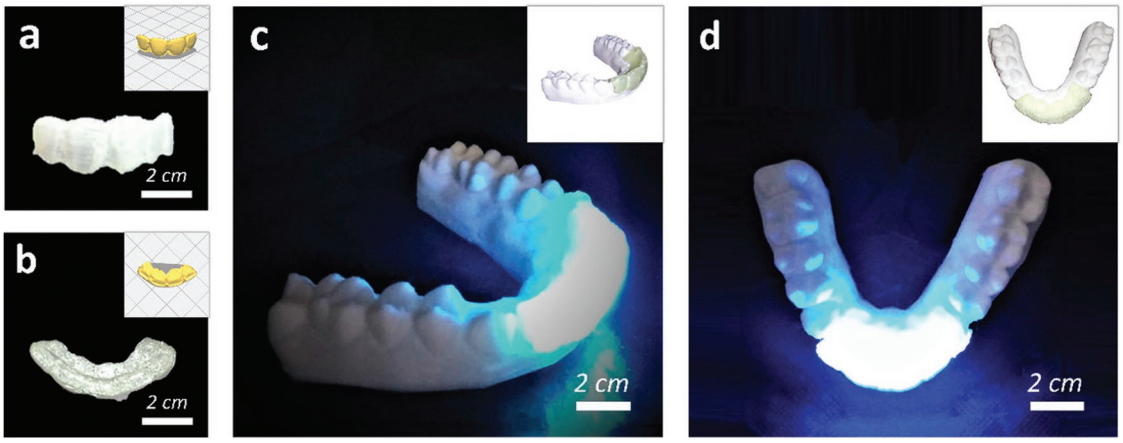

Figure 6. 3D printed random laser masks (RLMs) for photodynamical therapy. a) Printed RLM and the corresponding STL file in the front view. b) Printed RLM and the corresponding STL file in the top view. c) Laser emissions of the RLM attached seamlessly onto dentures in the side view. d) Laser emissions of the RLM attached seamlessly onto dentures in the top view.

samples is much larger than the wavelength of the random lasing by four to five orders of magnitude, the effect of the sample size on the lasing performance can be neglected. As a functional device for bioimaging, the 3D printed RLI needs to be precisely devised to meet the requirements of complex environments, and such a goal can be achieved by manipulating the printed patterns and structures. The fiber-like structure is designed to be easily placed into tissue and illuminate thicker or multilayer structures. To discuss the functionality of bioillumination and bioimaging, we gently introduced the device into chicken tissue (Figure 5c). The material biocompatibility of RLF has been proven, ensuring the possibility and validity for biological applications. PVA, as the printable matrix of RLF, holds several features such as bioadhesive capability, biodegradability, and swelling property.[42–44] Stilbene 420 is a derivative of stilbene family containing bioactive molecules extracted from edible plants;[45] TiO_2 particles have also been shown to exhibit highly desired properties for biocompatible coatings, cell-based substrates, point-of-care diagnostics, localized drug delivery,[46,47] etc. In Figure 5c, with the pumping energy tuned at 36 mJ cm^{-2}, the stimulated random laser emission effectively reaches the deep multilayer tissue through the fiber-like structure, contributing to the broad lightened area; even the grain of the muscle can be clearly observed. Based on random scattering, random laser systems endowed with laser-level intensity and isotropic emissions promise auspicious applicable values in speckle-free images, compensating for the congenital limitations of conventional lasers.[23] As shown in the top inset of Figure 5c, the microscopic image of the tissue can be efficiently investigated without suffering from coherence induced artifacts. The illuminated area grows larger and the tissue looks brighter as we pumped the RLI with higher PED at 50 mJ cm^{-2} (bottom inset of Figure 5c). In addition, due to the high solubility of PVA in water,[44,48] the RLI can exhibit dissolvability in bodies harmlessly within the prescribed time, allowing the capability of implantable photonics while circumventing reiterative surgeries for device replacement. To examine the transient and dissolvable abilities of the device, we immersed the entire device into physiological saline to mimic in vivo surroundings, and recorded photographs at different dissolving stages (Figure 5d). The outline began to blur within 30 min, and it was extremely difficult to identify the appearance of the whole device after 5 h, indicating the end of the dissolving process. It is believed that 3D printed implants for bioimaging will continue expanding the borders of biomedical research and inspiring much more far-reaching applications, spanning from morphological visualizing to clinical diagnosing to health monitoring.

Photodynamic therapy (PDT), one type of phototherapy, is a minimally invasive and clinically approved therapeutic modality that can exert cytotoxic activity toward target cells or tissue.[49,50] Upon irradiation with light of a suitable wavelength, the photosensitizers localized at the target region will be excited to higher energy states, react with the oxygenated environments, and generate reactive oxygen species leading to cell death.[50] In recent years, PDT has been evolved theoretically and clinically in several fields including cancer treatment, bacterial inactivation, antiviral therapy, and dermatological disorders.[51–54] **Figure 6** shows 3D printed random laser masks (RLMs) with extensive and customized functional areas, which can act as customized light sources for more diverse and specialized PDT in dentistry. Caries and inflammatory periodontitis, two of the most prevalent chronic diseases of oral cavities, are caused by pathogenic bacteria.[55,56] Conventional remedies such as endodontic treatment eradicate biofilm formation by mechanical root canal debridement and irrigation with antibacterial agents; however, invasive procedures need a longer recovery time, and the frequent use of antimicrobial agents may lead to drug resistance in oral bacteria.[57] Here, PDT can serve as a nonsurgical alternative against biofilm and plaque, and such a therapy coupled with 3D printing technology will open a new avenue for customized treatment without arduous procedures. To simulate the arbitrary distribution and extensive infection of biofilm, we design and formulate the RLM with free-form treated sites; the STL file and 3D printed result in different views are shown in Figure 6a,b. The RLM can be precisely printed according to the STL file even though the morphology of human teeth varies from person to person, ensuring the feasibility of personalized health care. In recent PDT research, lasers have an edge on large penetration depth and high energy efficiency among a variety of light sources

including arc lamps, fluorescent bulbs, and light-emitting diodes.[31] Nevertheless, due to the angle-dependent laser emission and limited laser beam size from meticulous setups, it is quite challenging to take conventional laser devices as efficient irradiance as caries and periodontitis are multi-localized or even widely spread. In stark contrast, the printed RLM with angle-free emissions in Figure 6c,d can be seamlessly attached on the teeth and covers any infective region. (More demonstrations of RLMs are provided in Figures S4–S7, Supporting Information.) The platform of 3D printed random lasers may further motivate more customized therapy in metastatic lesions, microorganism disinfection, and pathogen inactivation.

In summary, 3D printed random lasers can extend the borders of laser science as well as printing technology. 3D printing technique with great versatility, accessibility, and universality provides unprecedented opportunities for personalized laser devices for the general public. Moreover, based on the biodissolvability, biodegradability, and biocompatibility of the filament, 3D printed random lasers can be applied to speckle-free bioimages and large-scale phototherapy to observe and investigate multistructure and multifunction biotics, solving intriguing yet challenging issues from extremely complicated systems. It is foreseeable that the 3D printed random lasers developed here will be very useful in various fields including full-field imaging, microfluidic laser sensing, noninvasive phototherapeutic treating, and photonic lab-on-a-chip integrating.

Experimental Section

Random Laser Filament for FDM: Stilbene 420 (Exciton), TiO_2 particles, and poly(vinyl alcohol) were used as-purchased without further purification. First, the random laser materials, S420 and TiO_2 particles, and the thermoplastic matrix, PVA, were blended in the ratio of 1 g:200 mg:100 g. The mixture was combined at 50–70 rpm through the mixer and heated at 80 °C for 3 h in the hopper dryer. The powder-based precursor was loaded into the main chamber of the 50 mm single screw extruder, heated to 180 °C, and stirred at 150 rpm by a single screw drive auger coupled with a motor to attain the fused state. Next, the fused mixture was extruded through the nozzle at the speed of 20 m min^{-1} and sent through an air-cooling tunnel to solidify. Finally, the filament with the diameter of 1.75 mm was examined by a laser micrometer and collected as a roll. (More details about the optimization and fabrication are shown in Figures S8–S10, Supporting Information.)

Optical Measurements: To measure the random lasing action, the 3D printed samples were optically excited by frequency-quadrupled 266 nm pulsed Nd:YAG laser (NewWave, Tempest 300) with 4 ns pulse width and 10 Hz repetition. The energy of the single pulse shot is up to 200 mJ. The pumping beam was focused on a single spot by a cylindrical lens (f = 100 mm). A bandpass filter of 20 nm width was used to block the pump laser illumination. The emission properties were spectrally analyzed by means of a high-resolution spectrometer Jobin Yvon iHR550 with gratings of 300 and 1200 grooves per millimeter (spectral resolution 0.1 and 0.025 nm, respectively). A Synapse Thermoelectric Cooled CCD guaranteed to −75 °C was connected to the spectroscopy software SynerJY. The measuring angle in this setup was defined as the measured angle between the detector and the normal direction of the sample surface. All measurements were performed at room temperature.

Supporting Information

Supporting Information is available from the Wiley Online Library or from the author.

Acknowledgements

This work was supported by the Advanced Research Center of Green Materials Science and Technology through the grants funded by the Ministry of Education (107L9006) and the Ministry of Science and Technology (MOST 106-2112-M-005-010, 107-2218-E-005-021, and 107-3017-F-002-001), Taiwan. The authors thank Kuan-Jen Chen for the visual design and Yung-Ching Chang for providing molds for demonstrations.

Conflict of Interest

The authors declare no conflict of interest.

Author Contributions

Y.-T.H., Y.-Y.L., and Y.-Z.C. contributed equally to this work. Y.-T.H., H.-Y.L., Y.-M.L., and Y.-F.C. conceived the concept and wrote the manuscript. Y.-T.H., Y.-Y.L., Y.-Z.C., H.-Y.L., and C.-F.H. designed and conducted the experiments. Y.-T.H., Y.-Y.L., and Y.-Z.C. analyzed the data. H.-Y.L., M.-H.W., and W.-N.D. helped to solve the technical problems. Y.-F.C. supervised the project.

Keywords

3D printing optoelectronics, bioimaging implants, laser therapy, photonic filaments, random lasers

Received: August 29, 2019
Revised: October 20, 2019
Published online:

[1] S. J. Hollister, *Nat. Mater.* **2005**, *4*, 518.
[2] J. W. Jung, J. S. Lee, D. W. Cho, *Sci. Rep.* **2016**, *6*, 21685.
[3] J. T. Muth, D. M. Vogt, R. L. Truby, Y. Menguc, D. B. Kolesky, R. J. Wood, J. A. Lewis, *Adv. Mater.* **2014**, *26*, 6307.
[4] A. D. Valentine, T. A. Busbee, J. W. Boley, J. R. Raney, A. Chortos, A. Kotikian, J. D. Berrigan, M. F. Durstock, J. A. Lewis, *Adv. Mater.* **2017**, *29*, 1703817.
[5] M. S. Mannoor, Z. Jiang, T. James, Y. L. Kong, K. A. Malatesta, W. O. Soboyejo, N. Verma, D. H. Gracias, M. C. McAlpine, *Nano Lett.* **2013**, *13*, 2634.
[6] C. Cao, J. B. Andrews, A. D. Franklin, *Adv. Electron. Mater.* **2017**, *3*, 1700057.
[7] D. Vak, K. Hwang, A. Faulks, Y. S. Jung, N. Clark, D. Y. Kim, G. J. Wilson, S. E. Watkins, *Adv. Energy Mater.* **2015**, *5*, 1401539.
[8] L. van Dijk, U. W. Paetzold, G. A. Blab, R. E. Schropp, M. di Vece, *Prog. Photovoltaics* **2016**, *24*, 623.
[9] J. L. Demers, F. W. Esmonde-White, K. A. Esmonde-White, M. D. Morris, B. W. Pogue, *Biomed. Opt. Express* **2015**, *6*, 793.
[10] V. Saggiomo, A. H. Velders, *Adv. Sci.* **2015**, *2*, 1500125.
[11] A. K. Au, N. Bhattacharjee, L. F. Horowitz, T. C. Chang, A. Folch, *Lab Chip* **2015**, *15*, 1934.
[12] J. L. Erkal, A. Selimovic, B. C. Gross, S. Y. Lockwood, E. L. Walton, S. McNamara, R. S. Martin, D. M. Spence, *Lab Chip* **2014**, *14*, 2023.
[13] S. Nocentini, F. Riboli, M. Burresi, D. Martella, C. Parmeggiani, D. S. Wiersma, *ACS Photonics* **2018**, *5*, 3222.
[14] M. E. Staymates, W. A. MacCrehan, J. L. Staymates, R. R. Kunz, T. Mendum, T. H. Ong, G. Geurtsen, G. J. Gillen, B. A. Craven, *Sci. Rep.* **2016**, *6*, 36876.

[15] N. W. Bartlett, M. T. Tolley, J. T. Overvelde, J. C. Weaver, B. Mosadegh, K. Bertoldi, G. M. Whitesides, R. J. Wood, *Science* **2015**, *349*, 161.
[16] N. M. Lawandy, R. Balachandran, A. Gomes, E. Sauvain, *Nature* **1994**, *368*, 436.
[17] H. Cao, Y. G. Zhao, S. T. Ho, E. W. Seelig, Q. H. Wang, R. P. H. Chang, *Phys. Rev. Lett.* **1999**, *82*, 2278.
[18] D. S. Wiersma, *Nat. Phys.* **2008**, *4*, 359.
[19] R. C. Polson, Z. V. Vardeny, *Appl. Phys. Lett.* **2004**, *85*, 1289.
[20] W.-C. Liao, Y.-M. Liao, C.-T. Su, P. Perumal, S.-Y. Lin, W.-J. Lin, C.-H. Chang, H.-I. Lin, G. Haider, C.-Y. Chang, *ACS Appl. Nano Mater.* **2018**, *1*, 152.
[21] H. W. Hu, G. Haider, Y. M. Liao, P. K. Roy, R. Ravindranath, H. T. Chang, C. H. Lu, C. Y. Tseng, T. Y. Lin, W. H. Shih, Y. F. Chen, *Adv. Mater.* **2017**, *29*, 1703549.
[22] C. M. Raghavan, T.-P. Chen, S.-S. Li, W.-L. Chen, C.-Y. Lo, Y.-M. Liao, G. Haider, C.-C. Lin, C.-C. Chen, R. Sankar, *Nano Lett.* **2018**, *18*, 3221.
[23] B. Redding, M. A. Choma, H. Cao, *Nat. Photonics* **2012**, *6*, 355.
[24] Y. M. Liao, Y. C. Lai, P. Perumal, W. C. Liao, C. Y. Chang, C. S. Liao, S. Y. Lin, Y. F. Chen, *Adv. Mater. Technol.* **2016**, *1*, 1600068.
[25] Y. T. Hsu, C. T. Tai, H. M. Wu, C. F. Hou, Y. M. Liao, W. C. Liao, G. Haider, Y. C. Hsiao, C. W. Lee, S. W. Chang, Y. H. Chen, M. H. Wu, R. J. Chou, K. P. Bera, Y. Y. Lin, Y. Z. Chen, M. Kataria, S. Y. Lin, C. R. Paul Inbaraj, W. J. Lin, W. Y. Lee, T. Y. Lin, Y. C. Lai, Y. F. Chen, *ACS Nano* **2019**, *13*, 8977.
[26] Y. J. Lee, T. W. Yeh, Z. P. Yang, Y. C. Yao, C. Y. Chang, M. T. Tsai, J. K. Sheu, *Nanoscale* **2019**, *11*, 3534.
[27] B. Shivakiran Bhaktha, N. Bachelard, X. Noblin, P. Sebbah, *Appl. Phys. Lett.* **2012**, *101*, 151101.
[28] G. P. Luke, A. S. Hannah, S. Y. Emelianov, *Nano Lett.* **2016**, *16*, 2556.
[29] R. M. Gerosa, A. Sudirman, L. d. S. Menezes, W. Margulis, C. J. de Matos, *Optica* **2015**, *2*, 186.
[30] S. Balslev, A. Kristensen, *Opt. Express* **2005**, *13*, 344.
[31] M. Alexiades-Armenakas, *Clin. Dermatol.* **2006**, *24*, 16.
[32] S. J. Leigh, R. J. Bradley, C. P. Purssell, D. R. Billson, D. A. Hutchins, *PLoS One* **2012**, *7*, e49365.
[33] K. Fu, Y. Yao, J. Dai, L. Hu, *Adv. Mater.* **2017**, *29*, 1603486.
[34] H. Yuk, X. Zhao, *Adv. Mater.* **2018**, *30*, 1704028.
[35] O. A. Mohamed, S. H. Masood, J. L. Bhowmik, *Adv. Manuf.* **2015**, *3*, 42.
[36] O. S. Carneiro, A. F. Silva, R. Gomes, *Mater. Des.* **2015**, *83*, 768.
[37] G. van Soest, F. J. Poelwijk, R. Sprik, A. Lagendijk, *Phys. Rev. Lett.* **2001**, *86*, 1522.
[38] Y. Ling, H. Cao, A. L. Burin, M. A. Ratner, C. Liu, R. P. H. Chang, *Phys. Rev. A* **2001**, *64*, 063808.
[39] F. Luan, B. Gu, A. S. Gomes, K.-T. Yong, S. Wen, P. N. Prasad, *Nano Today* **2015**, *10*, 168.
[40] A. M. Smith, M. C. Mancini, S. Nie, *Nat. Nanotechnol.* **2009**, *4*, 710.
[41] Y. Yang, Q. Zhao, W. Feng, F. Li, *Chem. Rev.* **2013**, *113*, 192.
[42] T. Noguchi, T. Yamamuro, M. Oka, P. Kumar, Y. Kotoura, S. H. Hyon, Y. Ikada, *J. Appl. Biomater.* **1991**, *2*, 101.
[43] A. Chhatri, J. Bajpai, A. K. Bajpai, S. S. Sandhu, N. Jain, J. Biswas, *Carbohydr. Polym.* **2011**, *83*, 876.
[44] E. Chiellini, A. Corti, S. D'Antone, R. Solaro, *Prog. Polym. Sci.* **2003**, *28*, 963.
[45] B. Sun, A. M. Ribes, M. C. Leandro, A. P. Belchior, M. I. Spranger, *Anal. Chim. Acta* **2006**, *563*, 382.
[46] G. A. Crawford, N. Chawla, K. Das, S. Bose, A. Bandyopadhyay, *Acta Biomater.* **2007**, *3*, 359.
[47] R. Carbone, I. Marangi, A. Zanardi, L. Giorgetti, E. Chierici, G. Berlanda, A. Podesta, F. Fiorentini, G. Bongiorno, P. Piseri, P. G. Pelicci, P. Milani, *Biomaterials* **2006**, *27*, 3221.
[48] X. Shi, Y. M. Liao, H. Y. Lin, P. W. Tsao, M. J. Wu, S. Y. Lin, H. H. Hu, Z. Wang, T. Y. Lin, Y. C. Lai, Y. F. Chen, *ACS Nano* **2017**, *11*, 7600.
[49] T. J. Dougherty, C. J. Gomer, B. W. Henderson, G. Jori, D. Kessel, M. Korbelik, J. Moan, Q. Peng, *JNCI, J. Natl. Cancer Inst.* **1998**, *90*, 889.
[50] B. W. Henderson, T. J. Dougherty, *Photochem. Photobiol.* **1992**, *55*, 145.
[51] A. P. Castano, P. Mroz, M. R. Hamblin, *Nat. Rev. Cancer* **2006**, *6*, 535.
[52] N. S. Soukos, J. M. Goodson, *Periodontol. 2000* **2011**, *55*, 143.
[53] M. Wainwright, *Int. J. Antimicrob. Agents* **2003**, *21*, 510.
[54] P. Babilas, S. Schreml, M. Landthaler, R. M. Szeimies, *Photodermatol. Photoimmunol. Photomed.* **2010**, *26*, 118.
[55] S. S. Socransky, *J. Dent. Res.* **1970**, *49*, 203.
[56] J. A. Aas, B. J. Paster, L. N. Stokes, I. Olsen, F. E. Dewhirst, *J. Clin. Microbiol.* **2005**, *43*, 5721.
[57] C. B. Walker, *Periodontol. 2000* **1996**, *10*, 79.

